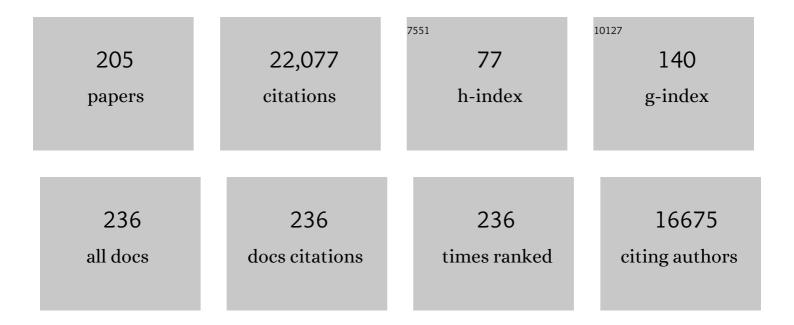
List of Publications by Year in descending order

Source: https://exaly.com/author-pdf/3359686/publications.pdf Version: 2024-02-01



#	Article	IF	CITATIONS
1	Atomic model of plant light-harvesting complex by electron crystallography. Nature, 1994, 367, 614-621.	13.7	2,012
2	The Resolution Revolution. Science, 2014, 343, 1443-1444.	6.0	986
3	Mechanisms of photoprotection and nonphotochemical quenching in pea light-harvesting complex at 2.5 â"« resolution. EMBO Journal, 2005, 24, 919-928.	3.5	731
4	Dimer ribbons of ATP synthase shape the inner mitochondrial membrane. EMBO Journal, 2008, 27, 1154-1160.	3.5	559
5	Biology, structure and mechanism of P-type ATPases. Nature Reviews Molecular Cell Biology, 2004, 5, 282-295.	16.1	498
6	Three-dimensional structure of plant light-harvesting complex determined by electron crystallography. Nature, 1991, 350, 130-134.	13.7	496
7	Structure and function of mitochondrial membrane protein complexes. BMC Biology, 2015, 13, 89.	1.7	459
8	Macromolecular organization of ATP synthase and complex I in whole mitochondria. Proceedings of the United States of America, 2011, 108, 14121-14126.	3.3	425
9	Structure of the yeast F <sub>1</sub> F <sub>o</sub> -ATP synthase dimer and its role in shaping the mitochondrial cristae. Proceedings of the National Academy of Sciences of the United States of America, 2012, 109, 13602-13607.	3.3	413
10	Lipid-protein Interactions in Crystals of Plant Light-harvesting Complex. Journal of Molecular Biology, 1993, 234, 347-356.	2.0	358
11	Three-dimensional structure of the plant photosystem II reaction centre at 8 à resolution. Nature, 1998, 396, 283-286.	13.7	340
12	Structure, mechanism, and regulation of the chloroplast ATP synthase. Science, 2018, 360, .	6.0	308
13	Two-dimensional crystallization of membrane proteins. Quarterly Reviews of Biophysics, 1992, 25, 1-49.	2.4	298
14	Aquaporin homologues in plants and mammals transport ammonia. FEBS Letters, 2004, 574, 31-36.	1.3	297
15	Horizontal membrane-intrinsic α-helices in the stator a-subunit of an F-type ATP synthase. Nature, 2015, 521, 237-240.	13.7	293
16	Arrangement of electron transport chain components in bovine mitochondrial supercomplex I <sub>1</sub> III <sub>2</sub> IV <sub>1</sub> . EMBO Journal, 2011, 30, 4652-4664.	3.5	290
17	Protein Insertion into the Mitochondrial Inner Membrane by a Twin-Pore Translocase. Science, 2003, 299, 1747-1751.	6.0	272
18	Cross-strand binding of TFAM to a single mtDNA molecule forms the mitochondrial nucleoid. Proceedings of the National Academy of Sciences of the United States of America, 2015, 112, 11288-11293.	3.3	266

#	Article	IF	CITATIONS
19	Structure and Mechanisms of F-Type ATP Synthases. Annual Review of Biochemistry, 2019, 88, 515-549.	5.0	266
20	Three-dimensional structure of the bacterial protein-translocation complex SecYEG. Nature, 2002, 418, 662-665.	13.7	237
21	Arrangement of Photosystem II and ATP Synthase in Chloroplast Membranes of Spinach and Pea Â. Plant Cell, 2010, 22, 1299-1312.	3.1	237
22	Structure of a Complete ATP Synthase Dimer Reveals the Molecular Basis of Inner Mitochondrial Membrane Morphology. Molecular Cell, 2016, 63, 445-456.	4.5	230
23	Amphipols From A to Z. Annual Review of Biophysics, 2011, 40, 379-408.	4.5	226
24	Cryo-EM enters a new era. ELife, 2014, 3, e03678.	2.8	214
25	Three-dimensional map of the plasma membrane H+-ATPase in the open conformation. Nature, 1998, 392, 840-843.	13.7	203
26	Age-dependent dissociation of ATP synthase dimers and loss of inner-membrane cristae in mitochondria. Proceedings of the National Academy of Sciences of the United States of America, 2013, 110, 15301-15306.	3.3	203
27	Three-dimensional structure of the light-harvesting chlorophyll a/b–protein complex. Nature, 1984, 307, 478-480.	13.7	196
28	Dimers of mitochondrial ATP synthase induce membrane curvature and self-assemble into rows. Proceedings of the National Academy of Sciences of the United States of America, 2019, 116, 4250-4255.	3.3	196
29	Protein denaturation at the air-water interface and how to prevent it. ELife, 2019, 8, .	2.8	196
30	Characterization of the translocon of the outer envelope of chloroplasts. Journal of Cell Biology, 2003, 160, 541-551.	2.3	195
31	Three-dimensional crystallization of membrane proteins. Quarterly Reviews of Biophysics, 1988, 21, 429-477.	2.4	182
32	Refolding of Escherichia coli produced membrane protein inclusion bodies immobilised by nickel chelating chromatography. FEBS Letters, 1998, 432, 21-26.	1.3	166
33	Rotary substates of mitochondrial ATP synthase reveal the basis of flexible F <sub>1</sub> -F <sub>o</sub> coupling. Science, 2019, 364, .	6.0	160
34	Two-dimensional structure of plant photosystem II at 8-Ã resolution. Nature, 1997, 389, 522-526.	13.7	159
35	Bacteriorhodopsin — the movie. Nature, 2000, 406, 569-570.	13.7	159
36	Structure of the monomeric outer-membrane porin OmpG in the open and closed conformation. EMBO Journal, 2006, 25, 3702-3713.	3.5	151

#	Article	IF	CITATIONS
37	Many wheels make light work. Nature, 1995, 374, 497-498.	13.7	142
38	Cryo-EM Structure of the TOM Core Complex from Neurospora crassa. Cell, 2017, 170, 693-700.e7.	13.5	138
39	Sequence conservation of light-harvesting and stress-response proteins in relation to the three-dimensional molecular structure of LHCII. Photosynthesis Research, 1995, 44, 139-148.	1.6	136
40	Atomic model of the F420-reducing [NiFe] hydrogenase by electron cryo-microscopy using a direct electron detector. ELife, 2014, 3, e01963.	2.8	132
41	Functional asymmetry and electron flow in the bovine respirasome. ELife, 2016, 5, .	2.8	130
42	Projection structure and oligomeric properties of a bacterial core protein translocase. EMBO Journal, 2001, 20, 2462-2471.	3.5	126
43	Crystallisation, structure and function of plant light-harvesting Complex II. Biochimica Et Biophysica Acta - Bioenergetics, 2009, 1787, 753-772.	0.5	126
44	Structure and autoregulation of a P4-ATPase lipid flippase. Nature, 2019, 571, 366-370.	13.7	126
45	Protein translocase of the outer mitochondrial membrane: role of import receptors in the structural organization of the TOM complex. Journal of Molecular Biology, 2002, 316, 657-666.	2.0	123
46	Central Role of Mic10 in the Mitochondrial Contact Site and Cristae Organizing System. Cell Metabolism, 2015, 21, 747-755.	7.2	120
47	CryoEM structures of membrane pore and prepore complex reveal cytolytic mechanism of Pneumolysin. ELife, 2017, 6, .	2.8	119
48	Conserved in situ arrangement of complex I and III <sub>2</sub> in mitochondrial respiratory chain supercomplexes of mammals, yeast, and plants. Proceedings of the National Academy of Sciences of the United States of America, 2018, 115, 3024-3029.	3.3	119
49	Molecular Architecture of the Undecameric Rotor of a Bacterial Na+-ATP Synthase. Journal of Molecular Biology, 2002, 321, 307-316.	2.0	118
50	High-resolution electron crystallography of light-harvesting chlorophyll -protein complex in three different media. Journal of Molecular Biology, 1991, 217, 691-699.	2.0	116
51	Crystal structure of listeriolysin O reveals molecular details of oligomerization and pore formation. Nature Communications, 2014, 5, 3690.	5.8	116
52	Structure, Mechanism, and Regulation of the Neurospora Plasma Membrane H+-ATPase. Science, 2002, 297, 1692-1696.	6.0	115
53	Mutant Trimers of Light-Harvesting Complex II Exhibit Altered Pigment Content and Spectroscopic Featuresâ€. Biochemistry, 1999, 38, 16214-16222.	1.2	114
54	Projection structure of NhaA, a secondary transporter from Escherichia coli, at 4.0 A resolution. EMBO Journal, 1999, 18, 3558-3563.	3.5	113

#	Article	IF	CITATIONS
55	The state of detergent solubilised light-harvesting chlorophyll-a/b protein complex as monitored by picosecond time-resolved fluorescence and circular dichroism. Biochimica Et Biophysica Acta - Bioenergetics, 1987, 893, 349-364.	0.5	110
56	Spectroscopic characterization of three different monomeric forms of the main chlorophyll a/b binding protein from chloroplast membranes. Biochemistry, 1994, 33, 14775-14783.	1.2	110
57	Structural basis of Na+-independent and cooperative substrate/product antiport in CaiT. Nature, 2010, 467, 233-236.	13.7	110
58	High-resolution cryo-EM structures of respiratory complex I: Mechanism, assembly, and disease. Science Advances, 2019, 5, eaax9484.	4.7	109
59	Crystal structure of plant light-harvesting complex shows the active, energy-transmitting state. EMBO Journal, 2009, 28, 298-306.	3.5	108
60	Changes of mitochondrial ultrastructure and function during ageing in mice and Drosophila. ELife, 2017, 6, .	2.8	108
61	Molecular insights into lipid-assisted Ca2+ regulation of the TRP channel Polycystin-2. Nature Structural and Molecular Biology, 2017, 24, 123-130.	3.6	105
62	Structure of a type IV pilus machinery in the open and closed state. ELife, 2015, 4, .	2.8	103
63	Structure and function of the plant light-harvesting complex, LHC-II. Current Opinion in Structural Biology, 1994, 4, 519-528.	2.6	101
64	Controlled Unfolding and Refolding of a Single Sodium-proton Antiporter using Atomic Force Microscopy. Journal of Molecular Biology, 2004, 340, 1143-1152.	2.0	99
65	Direct interaction of the major light-harvesting complex II and PsbS in nonphotochemical quenching. Proceedings of the National Academy of Sciences of the United States of America, 2013, 110, 5452-5456.	3.3	98
66	Cryo-EM structure of respiratory complex I at work. ELife, 2018, 7, .	2.8	98
67	The structure of membrane crystals of the light-harvesting chlorophyll a/b protein complex Journal of Cell Biology, 1983, 96, 1414-1424.	2.3	97
68	Electron tomography of plant thylakoid membranes. Journal of Experimental Botany, 2011, 62, 2393-2402.	2.4	96
69	Structure and substrate ion binding in the sodium/proton antiporter PaNhaP. ELife, 2014, 3, e03579.	2.8	92
70	Loss of LRPPRC causes ATP synthase deficiency. Human Molecular Genetics, 2014, 23, 2580-2592.	1.4	91
71	Structure of outer membrane protein G in lipid bilayers. Nature Communications, 2017, 8, 2073.	5.8	91
72	Active site rearrangement and structural divergence in prokaryotic respiratory oxidases. Science, 2019, 366, 100-104.	6.0	90

#	Article	IF	CITATIONS
73	Assignment of Spectral Substructures to Pigment-Binding Sites in Higher Plant Light-Harvesting Complex LHC-IIâ€. Biochemistry, 2002, 41, 2281-2287.	1.2	89
74	A mitofusin-dependent docking ring complex triggers mitochondrial fusion in vitro. ELife, 2016, 5, .	2.8	87
75	Structure and assembly of the mitochondrial membrane remodelling GTPase Mgm1. Nature, 2019, 571, 429-433.	13.7	86
76	Locating ligand binding and activation of a single antiporter. EMBO Reports, 2005, 6, 668-674.	2.0	85
77	Cryo-Electron Microscopy Structure of a Yeast Mitochondrial Preprotein Translocase. Journal of Molecular Biology, 2008, 383, 1049-1057.	2.0	83
78	Structure and in situ organisation of the Pyrococcus furiosus archaellum machinery. ELife, 2017, 6, .	2.8	83
79	Outer membrane continuity and septosome formation between vegetative cells in the filaments of Anabaena sp. PCC 7120. Cellular Microbiology, 2011, 13, 1744-1754.	1.1	81
80	Evidence for Structural Integrity in the Undecameric c-Rings Isolated from Sodium ATP Synthases. Journal of Molecular Biology, 2003, 325, 389-397.	2.0	80
81	Chloroplast Omp85 proteins change orientation during evolution. Proceedings of the National Academy of Sciences of the United States of America, 2011, 108, 13841-13846.	3.3	80
82	Solid-State Magic-Angle Spinning NMR of Outer-Membrane Protein G from Escherichia coli. ChemBioChem, 2005, 6, 1679-1684.	1.3	79
83	Distribution of RNA and protein in crystalline eukaryotic ribosomes. Journal of Molecular Biology, 1982, 156, 431-448.	2.0	78
84	Rotary ATPases: A New Twist to an Ancient Machine. Trends in Biochemical Sciences, 2016, 41, 106-116.	3.7	78
85	The Three Isoforms of the Light-harvesting Complex II. Journal of Biological Chemistry, 2004, 279, 36884-36891.	1.6	77
86	Two-dimensional structure of light harvesting complex II (LHII) from the purple bacterium Rhodovulum sulfidophilum and comparison with LHII from Rhodopseudomonas acidophila. Structure, 1996, 4, 243-252.	1.6	75
87	Membrane perforation by the pore-forming toxin pneumolysin. Proceedings of the National Academy of Sciences of the United States of America, 2019, 116, 13352-13357.	3.3	75
88	Structure and transport mechanism of the sodium/proton antiporter MjNhaP1. ELife, 2014, 3, e03583.	2.8	73
89	Two-dimensional structure of plant light-harvesting complex at 37 Ã resolution by electron crystallography. Journal of Molecular Biology, 1989, 207, 823-828.	2.0	72
90	Carotenoid Radical Cations as a Probe for the Molecular Mechanism of Nonphotochemical Quenching in Oxygenic Photosynthesis. Journal of Physical Chemistry B, 2007, 111, 3481-3487.	1.2	71

#	Article	IF	CITATIONS
91	Bovine F1Fo ATP synthase monomers bend the lipid bilayer in 2D membrane crystals. ELife, 2015, 4, e06119.	2.8	71
92	Projection Structure of Channelrhodopsin-2 at 6ÂÃ Resolution by Electron Crystallography. Journal of Molecular Biology, 2011, 414, 86-95.	2.0	70
93	Two-dimensional crystallization of a membrane protein on a detergent-resistant lipid monolayer 1 1Edited by R. Huber. Journal of Molecular Biology, 2001, 308, 639-647.	2.0	68
94	First Insights into the Entry Process of Hyperthermophilic Archaeal Viruses. Journal of Virology, 2013, 87, 13379-13385.	1.5	66
95	High-resolution structure and dynamics of mitochondrial complex l—Insights into the proton pumping mechanism. Science Advances, 2021, 7, eabj3221.	4.7	65
96	Photosystem II. Current Opinion in Structural Biology, 1999, 9, 469-475.	2.6	64
97	Accumulation of plant antenna complexes is regulated by post-transcriptional mechanisms in tobacco Plant Cell, 1995, 7, 149-160.	3.1	63
98	Structure of the SecY Complex Unlocked by a Preprotein Mimic. Cell Reports, 2012, 1, 21-28.	2.9	63
99	Direct structural insight into the substrate-shuttling mechanism of yeast fatty acid synthase by electron cryomicroscopy. Proceedings of the National Academy of Sciences of the United States of America, 2010, 107, 9164-9169.	3.3	62
100	Helical arrays of U-shaped ATP synthase dimers form tubular cristae in ciliate mitochondria. Proceedings of the National Academy of Sciences of the United States of America, 2016, 113, 8442-8447.	3.3	62
101	Visualizing active membrane protein complexes by electron cryotomography. Nature Communications, 2014, 5, 4129.	5.8	59
102	Structural basis of proton translocation and force generation in mitochondrial ATP synthase. ELife, 2017, 6, .	2.8	59
103	Consensus Structural Features of Purified Bacterial TatABC Complexes. Journal of Molecular Biology, 2003, 330, 277-286.	2.0	58
104	Mechanism of Na+-dependent citrate transport from the structure of an asymmetrical CitS dimer. ELife, 2015, 4, e09375.	2.8	58
105	Structure of GlnK1 with bound effectors indicates regulatory mechanism for ammonia uptake. EMBO Journal, 2007, 26, 589-599.	3.5	57
106	Three-dimensional crystals of the light-harvesting chlorophyll protein complex from pea chloroplasts. Journal of Molecular Biology, 1987, 194, 757-762.	2.0	54
107	pH-induced structural change in a sodium/proton antiporter from Methanococcus jannaschii. EMBO Journal, 2005, 24, 2720-2729.	3.5	54
108	Correlation of Car S <sub>1</sub> → Chl with Chl → Car S <sub>1</sub> Energy Transfer Supports the Excitonic Model in Quenched Light Harvesting Complex II. Journal of Physical Chemistry B, 2010, 114, 15650-15655.	1.2	54

#	Article	IF	CITATIONS
109	Structure of the archaeal Na+/H+antiporter NhaP1 and functional role of transmembrane helix 1. EMBO Journal, 2011, 30, 439-449.	3.5	54
110	CryoEM at <b>IUCrJ</b> : a new era. IUCrJ, 2016, 3, 3-7.	1.0	54
111	Electron cryo-microscopy of biological specimens on conductive titanium–silicon metal glass films. Ultramicroscopy, 2008, 108, 698-705.	0.8	52
112	A ferredoxin bridge connects the two arms of plant mitochondrial complex I. Plant Cell, 2021, 33, 2072-2091.	3.1	52
113	Effect of surface roughness of carbon support films on high-resolution electron diffraction of two-dimensional protein crystals. Ultramicroscopy, 1991, 36, 307-318.	0.8	51
114	Discrimination of protein and nucleic acids by electron microscopy using contrast variation. Ultramicroscopy, 1982, 7, 221-231.	0.8	50
115	Cyclophilin D links programmed cell death and organismal aging in <i>Podospora anserina</i> . Aging Cell, 2010, 9, 761-775.	3.0	50
116	In situ structure of trypanosomal ATP synthase dimer reveals a unique arrangement of catalytic subunits. Proceedings of the National Academy of Sciences of the United States of America, 2017, 114, 992-997.	3.3	49
117	Observing Folding Pathways and Kinetics of a Single Sodium-proton Antiporter from Escherichia coli. Journal of Molecular Biology, 2006, 355, 2-8.	2.0	48
118	[2,3-13C]-labeling of Aromatic ResiduesGetting a Head Start in the Magic-Angle-Spinning NMR Assignment of Membrane Proteins. Journal of the American Chemical Society, 2008, 130, 408-409.	6.6	48
119	pH-Induced Conformational Change of the β-Barrel-Forming Protein OmpG Reconstituted into Native E. coli Lipids. Journal of Molecular Biology, 2010, 396, 610-616.	2.0	48
120	Structure of Human Na+/H+ Exchanger NHE1 Regulatory Region in Complex with Calmodulin and Ca2+. Journal of Biological Chemistry, 2011, 286, 40954-40961.	1.6	47
121	A 3D cellular context for the macromolecular world. Nature Structural and Molecular Biology, 2014, 21, 841-845.	3.6	47
122	The crystal structure of an orthorhombic form of adenosine-5'-monophosphate. Acta Crystallographica Section B: Structural Crystallography and Crystal Chemistry, 1976, 32, 1850-1855.	0.4	46
123	Structure of light-harvesting chlorophyll protein complex from plant photosynthetic membranes at 7 à resolution in projection. Journal of Molecular Biology, 1988, 202, 849-864.	2.0	46
124	Projection Structure and Oligomeric State of the Osmoregulated Sodium/Glycine Betaine Symporter BetP of Corynebacterium glutamicum. Journal of Molecular Biology, 2004, 337, 1137-1147.	2.0	45
125	Self-assembly of the general membrane-remodeling protein PVAP into sevenfold virus-associated pyramids. Proceedings of the National Academy of Sciences of the United States of America, 2014, 111, 3829-3834.	3.3	45
126	Comparison of H+-ATPase and Ca2+-ATPase suggests that a large conformational change initiates P-type ion pump reaction cycles. Current Biology, 1999, 9, 672-679.	1.8	44

#	Article	IF	CITATIONS
127	Structure of the P-type ATPases. Current Opinion in Structural Biology, 1998, 8, 510-516.	2.6	43
128	Projection Structure of yidC: A Conserved Mediator of Membrane Protein Assembly. Journal of Molecular Biology, 2008, 375, 901-907.	2.0	42
129	Light-Induced Helix Movements in Channelrhodopsin-2. Journal of Molecular Biology, 2015, 427, 341-349.	2.0	42
130	Projection structure of the monomeric porin OmpG at 6 å resolution. Journal of Molecular Biology, 2001, 305, 71-77.	2.0	41
131	Conformations of NhaA, the Na/H Exchanger from Escherichia coli, in the pH-Activated and Ion-Translocating States. Journal of Molecular Biology, 2009, 386, 351-365.	2.0	40
132	Surface crystallisation of the plasma membrane H+-ATPase on a carbon support film for electron crystallography. Journal of Molecular Biology, 1999, 287, 961-968.	2.0	39
133	Molecular architecture of the Nâ€ŧype <scp>ATP</scp> ase rotor ring from <i>Burkholderia pseudomallei</i> . EMBO Reports, 2017, 18, 526-535.	2.0	39
134	The 3.7 Ã projection map of the glycerol facilitator GlpF: a variant of the aquaporin tetramer. EMBO Reports, 2000, 1, 183-189.	2.0	38
135	One βâ€Hairpin after the Other: Exploring Mechanical Unfolding Pathways of the Transmembrane βâ€Barrel Protein OmpG. Angewandte Chemie - International Edition, 2009, 48, 8306-8308.	7.2	38
136	Structural basis for energy transduction by respiratory alternative complex III. Nature Communications, 2018, 9, 1728.	5.8	38
137	pH-Dependent Interactions Guide the Folding and Gate the Transmembrane Pore of the Î <sup>2</sup> -Barrel Membrane Protein OmpG. Journal of Molecular Biology, 2010, 397, 878-882.	2.0	37
138	Keeping It Simple, Transport Mechanism and pH Regulation in Na+/H+ Exchangers. Journal of Biological Chemistry, 2014, 289, 13168-13176.	1.6	37
139	Structure and Function of Prokaryotic Glutamate Transporters fromEscherichia coli and Pyrococcus horikoshiiâ€. Biochemistry, 2006, 45, 12796-12805.	1.2	35
140	Chlorophyllbis involved in long-wavelength spectral properties of light-harvesting complexes LHC I and LHC II. FEBS Letters, 2001, 499, 27-31.	1.3	34
141	Analysis of macromolecular structure and dynamics by electron cryo-microscopy. Current Opinion in Chemical Biology, 1999, 3, 537-543.	2.8	32
142	Human Leukotriene C4 Synthase at 4.5 Ã Resolution in Projection. Structure, 2004, 12, 2009-2014.	1.6	32
143	A comparison of the three isoforms of the light-harvesting complex II using transient absorption and time-resolved fluorescence measurements. Photosynthesis Research, 2006, 88, 269-285.	1.6	32
144	Protein Dynamics Tunes Excited State Positions in Light-Harvesting Complex II. Journal of Physical Chemistry B, 2015, 119, 3920-3930.	1.2	32

#	Article	IF	CITATIONS
145	Supramolecular organization of the human N-BAR domain in shaping the sarcolemma membrane. Journal of Structural Biology, 2016, 194, 375-382.	1.3	32
146	Mechanism of the electroneutral sodium/proton antiporter PaNhaP from transition-path shooting. Nature Communications, 2019, 10, 1742.	5.8	32
147	The 6.9-Ã Structure of ClpF: A Basis for Homology Modeling of the Glycerol Channel from Escherichia coli. Journal of Structural Biology, 2000, 132, 133-141.	1.3	30
148	Oligomeric Structure of the Carnitine Transporter CaiT from Escherichia coli. Journal of Biological Chemistry, 2006, 281, 4795-4801.	1.6	30
149	Structural Asymmetry in a Trimeric Na+/Betaine Symporter, BetP, from Corynebacterium glutamicum. Journal of Molecular Biology, 2011, 407, 368-381.	2.0	30
150	Large scale expression, purification and 2D crystallization of recombinant plant plasma membrane H+-ATPase. Journal of Molecular Biology, 2001, 309, 465-476.	2.0	29
151	Properties of zeaxanthin and its radical cation bound to the minor light-harvesting complexes CP24, CP26 and CP29. Biochimica Et Biophysica Acta - Bioenergetics, 2009, 1787, 747-752.	0.5	29
152	Structure and function of bacterial light-harvesting complexes. Structure, 1995, 3, 521-525.	1.6	28
153	Correlation between the OmpG Secondary Structure and Its pH-Dependent Alterations Monitored by FTIR. Journal of Molecular Biology, 2010, 401, 56-67.	2.0	28
154	Energy-filtered transmission electron microscopy of biological samples on highly transparent carbon nanomembranes. Ultramicroscopy, 2011, 111, 342-349.	0.8	28
155	Membrane Structure of CtrA3, a Copper-transporting P-type-ATPase from Aquifex aeolicus. Journal of Molecular Biology, 2008, 378, 581-595.	2.0	27
156	Structure and Function of the FeoB G-Domain from Methanococcus jannaschii. Journal of Molecular Biology, 2009, 392, 405-419.	2.0	27
157	Cryo-EM structure of respiratory complex I reveals a link to mitochondrial sulfur metabolism. Biochimica Et Biophysica Acta - Bioenergetics, 2016, 1857, 1935-1942.	0.5	27
158	Cryo-EM structure of the bifunctional secretin complex of Thermus thermophilus. ELife, 2017, 6, .	2.8	27
159	Molecular landscape of etioplast inner membranes in higher plants. Nature Plants, 2021, 7, 514-523.	4.7	27
160	High-resolution electron microscopy of biological specimens in cubic ice. Ultramicroscopy, 1994, 55, 141-153.	0.8	26
161	In-focus electron microscopy of frozen-hydrated biological samples with a Boersch phase plate. Ultramicroscopy, 2011, 111, 1696-1705.	0.8	26
162	Visualization of ATP Synthase Dimers in Mitochondria by Electron Cryo-tomography. Journal of Visualized Experiments, 2014, , 51228.	0.2	26

#	Article	IF	CITATIONS
163	Chlorophylls galore. Nature, 2001, 411, 897-899.	13.7	25
164	High-yield Expression, Reconstitution and Structure of the Recombinant, Fully Functional Glutamate Transporter GLT-1 from Rattus norvegicus. Journal of Molecular Biology, 2005, 351, 598-613.	2.0	25
165	Two-dimensional crystallization of human vitamin K-dependent γ-glutamyl carboxylase. Journal of Structural Biology, 2007, 157, 437-442.	1.3	25
166	Three-dimensional electron diffraction of plant light-harvesting complex. Biophysical Journal, 1992, 61, 287-297.	0.2	22
167	Current limitations to high-resolution structure determination by single-particle cryoEM. Quarterly Reviews of Biophysics, 2021, 54, e4.	2.4	21
168	Structural differences in the inner part of Photosystem II between higher plants and cyanobacteria. Photosynthesis Research, 2005, 85, 3-13.	1.6	20
169	Devitrification reduces beam-induced movement in cryo-EM. IUCrJ, 2021, 8, 186-194.	1.0	20
170	Structure of the hexameric fungal plasma membrane proton pump in its autoinhibited state. Science Advances, 2021, 7, eabj5255.	4.7	20
171	Forty years in cryoEM of membrane proteins. Microscopy (Oxford, England), 2022, 71, i30-i50.	0.7	20
172	Arginine oscillation explains Na <sup>+</sup> independence in the substrate/product antiporter CaiT. Proceedings of the National Academy of Sciences of the United States of America, 2013, 110, 17296-17301.	3.3	19
173	GRecon: A Method for the Lipid Reconstitution of Membrane Proteins. Angewandte Chemie - International Edition, 2012, 51, 8343-8347.	7.2	17
174	Purification and two-dimensional crystallization of highly active cytochrome b 6 f complex from spinach. FEBS Letters, 1999, 463, 97-102.	1.3	16
175	Dual energy landscape: The functional state of the βâ€barrel outer membrane protein G molds its unfolding energy landscape. Proteomics, 2010, 10, 4151-4162.	1.3	16
176	Self-Perforated Hydrogel Nanomembranes Facilitate Structural Analysis of Proteins by Electron Cryo-Microscopy. ACS Nano, 2017, 11, 6467-6473.	7.3	16
177	The resolution revolution in cryoEM requires high-quality sample preparation: a rapid pipeline to a high-resolution map of yeast fatty acid synthase. IUCrJ, 2020, 7, 220-227.	1.0	16
178	Heterologously Expressed GLT-1 Associates in â^¼200-nm Protein-Lipid Islands. Biophysical Journal, 2006, 91, 3718-3726.	0.2	15
179	Electrogenic Cation Binding in the Electroneutral Na+/H+ Antiporter of Pyrococcus abyssi. Journal of Biological Chemistry, 2016, 291, 26786-26793.	1.6	15
180	Practical aspects of Boersch phase contrast electron microscopy of biological specimens. Ultramicroscopy, 2012, 116, 62-72.	0.8	14

#	Article	IF	CITATIONS
181	Towards an optimum design for electrostatic phase plates. Ultramicroscopy, 2015, 153, 22-31.	0.8	14
182	Dual approach to a light problem. Nature, 2003, 426, 399-400.	13.7	13
183	A ribonucleoprotein core in the 50 S ribosomal subunit of Escherichia coli. FEBS Letters, 1978, 94, 207-212.	1.3	12
184	Single-walled carbon nanotubes and nanocrystalline graphene reduce beam-induced movements in high-resolution electron cryo-microscopy of ice-embedded biological samples. Applied Physics Letters, 2011, 99, .	1.5	12
185	Separation of phosphorylated and unphosphorylated light-harvesting chlorophyll ab-protein complex by column chromatography. Biochimica Et Biophysica Acta - Bioenergetics, 1988, 934, 118-122.	0.5	9
186	Introduction to Electron Crystallography. Methods in Molecular Biology, 2013, 955, 1-16.	0.4	9
187	Infrared spectroscopic study of the structural and functional properties of the Na+/H+ antiporter MjNhaP1 from Methanococcus jannaschii. Biochimica Et Biophysica Acta - Bioenergetics, 2009, 1787, 730-737.	0.5	8
188	Noncovalent Functionalization of Carbon Substrates with Hydrogels Improves Structural Analysis of Vitrified Proteins by Electron Cryo-Microscopy. ACS Nano, 2019, 13, 7185-7190.	7.3	8
189	Ion Binding and Selectivity of the Na <sup>+</sup> /H <sup>+</sup> Antiporter MjNhaP1 from Experiment and Simulation. Journal of Physical Chemistry B, 2020, 124, 336-344.	1.2	8
190	Light-Induced Changes in the Chemical Bond Structure of Light-Harvesting Complex II Probed by FTIR Spectroscopyâ€. Biochemistry, 2003, 42, 10223-10228.	1.2	7
191	Purification, crystallization and preliminary X-ray diffraction analysis of the FeoB G domain from <i>Methanococcus jannaschii</i> . Acta Crystallographica Section F: Structural Biology Communications, 2009, 65, 684-687.	0.7	6
192	Chlorophyll dichroism of three-dimensional crystals of the light-harvesting chlorophyll a /b -protein complex. FEBS Letters, 1988, 226, 275-279.	1.3	5
193	Three in a row—how sodium ions cross the channel. EMBO Journal, 2016, 35, 793-795.	3.5	5
194	Conformational changes in the yeast mitochondrial ABC transporter Atm1 during the transport cycle. Science Advances, 2021, 7, eabk2392.	4.7	4
195	Pumping ions. Nature Structural Biology, 1997, 4, 773-773.	9.7	3
196	Structure Of The Mitochondrial ATP Synthase And Its Role In Shaping Mitochondria Cristae. Microscopy and Microanalysis, 2012, 18, 56-57.	0.2	3
197	Structure of the catalytic F <sub>1</sub> head of the F <sub>1</sub> -F <sub>o</sub> ATP synthase from <i>Trypanosoma brucei</i> . Proceedings of the National Academy of Sciences of the United States of America, 2018, 115, E2906-E2907.	3.3	3
198	Cryo-EM structure of <i>Neurospora crassa</i> respiratory complex IV. IUCrJ, 2019, 6, 773-780.	1.0	3

#	Article	IF	CITATIONS
199	Ca2+-mediated higher-order assembly of heterodimers in amino acid transport system b0,+ biogenesis and cystinuria. Nature Communications, 2022, 13, 2708.	5.8	3
200	Membrane proteins. Current Opinion in Structural Biology, 1991, 1, 531-533.	2.6	1
201	Membrane proteins. Current Opinion in Structural Biology, 1993, 3, 499-500.	2.6	1
202	Another Phase Plate in the Zoo: Reducing Charging and Optimizing the Design of Electrostatic Phase Plates. Microscopy and Microanalysis, 2015, 21, 1941-1942.	0.2	1
203	Reply to Desikan et al.: Micelle formation among various mechanisms of toxin pore formation. Proceedings of the National Academy of Sciences of the United States of America, 2020, 117, 5109-5110.	3.3	1
204	Detergent effects upon the picosecond dynamics of higher-plant light-harvesting chlorophyll complex (LHC2). Journal of the Chemical Society, Faraday Transactions 2, 1986, 82, 2263.	1.1	0
205	CryoEM structures of ATP synthase. Biochimica Et Biophysica Acta - Bioenergetics, 2018, 1859, e3-e4.	0.5	0